Electronic Supplementary Information

Superwetting charged copper foams with long permeation channels for ultrafast emulsion separation and surfactant removal†

Jihao Zuo,[a] Zehao Chen,[a] Yi Zhou,[a] Zihan Liu,[a] Cailong Zhou,[b] Shouping Xu,[a] Jiang Cheng,[a] Xiufang Wen*[a] and Pihui Pi*[a]

* Corresponding authors

[a] School of Chemistry and Chemical Engineering, Guangdong Provincial Key Lab of Green Chemical Product Technology, Guangdong Engineering Technology Research Center of Advanced Insulating Coating, South China University of Technology, Guangzhou 510640, P. R. China

E-mail: xfwen@scut.edu.cn, phpi@scut.edu.cn

[b] School of Chemistry and Chemical Engineering, Chongqing University, Chongqing 400044, P. R. China

Supplementary Figure and Movie Captions

Fig. S1 Schematic representation for (a) preparation of CF-$Cu(OH)_2$ *via* a three-electrode anodization reaction and the corresponding electrochemical reaction equation. Schematic representation of directional electric field driven assembly method for (b) preparation of CF-$Cu(OH)_2$@CNTs-NH_2 *via* the assembly of CNTs-NH_2 on CF-$Cu(OH)_2$ and (c) preparation of CF-$Cu(OH)_2$@CNTs-COOH *via* the assembly of CNTs-COOH on CF-$Cu(OH)_2$.

Fig. S2 Digital pictures of the pristine copper foam, CF-$Cu(OH)_2$, CF-$Cu(OH)_2$@CNTs-NH_2 and CF-$Cu(OH)_2$@CNTs-COOH.

Fig. S3 XRD pattern of the CF-$Cu(OH)_2$.

Fig. S4 (a) The SEM image of multilevel cage-like architecture for the copper foam. (b) Schematic illustration of the assembly of CNTs-NH_2 on the CF-$Cu(OH)_2$ *via* directional electric field driven assembly method. (c) The diagram of exterior area and interior area of the CF-$Cu(OH)_2$@CNTs-NH_2.

Fig. S5 The effect of concentration of CNTs solution on loading amount of CNTs of the (a) CF-$Cu(OH)_2$@CNTs-NH_2 and (b) CF-$Cu(OH)_2$@CNTs-COOH (The electric field assembly time of CF-$Cu(OH)_2$@CNTs-NH_2 and CF-$Cu(OH)_2$@CNTs-COOH were fixed at 15 min and 5 min, respectively).

Fig. S6 The effect of electric field assembly time on loading amount of CNTs of the (a) CF-$Cu(OH)_2$@CNTs-NH_2 and (b) CF-$Cu(OH)_2$@CNTs-COOH (The concentrations of CNTs-NH_2/ CNTs-COOH solution in the assembly process for CF-$Cu(OH)_2$@CNTs-NH_2 and CF-$Cu(OH)_2$@CNTs-COOH were all fixed at 1 $g \cdot L^{-1}$).

Fig. S7 SEM images of (a) CF-$Cu(OH)_2$@CNTs-NH_2 assembled with 0.1 $g \cdot L^{-1}$ CNTs-NH_2 solution for 15 min, (b) CF-$Cu(OH)_2$@CNTs-COOH assembled with 0.1 $g \cdot L^{-1}$ CNTs-COOH solution for 5 min.

Fig. S8 SEM images of (a) CF-$Cu(OH)_2$@CNTs-NH_2 assembled with 5 $g \cdot L^{-1}$ CNTs-NH_2 solution for 15 min, (b) CF-$Cu(OH)_2$@CNTs-COOH assembled with 5 $g \cdot L^{-1}$ CNTs-COOH solution for 5 min.

Fig. S9 The EDS mapping for (a) CF-$Cu(OH)_2$@CNTs-NH_2 and (b) CF-$Cu(OH)_2$@CNTs-COOH.

Fig. S10 The water contact angle (WCA), oil contact angle (OCA) and underwater oil contact angle (UWOCA) of (a) pristine copper foam and (b) CF-$Cu(OH)_2$.

Fig. S11 The measurement of oil intrusion pressures of 30 pieces of CF-$Cu(OH)_2$@CNTs-NH_2 and 25 pieces of CF-$Cu(OH)_2$@CNTs-COOH (Oil are toluene (red) and 1,2-dichloroethane (purple)).

Fig. S12 (a) The appearance of the filtrates for SDS-T/W emulsion separated by CF-$Cu(OH)_2$@CNTs-NH_2 with different numbers (1, 5, 10, 15, 20, 25 and 30). (b) The appearance of the filtrates for DTAC-T/W emulsion separated by CF-$Cu(OH)_2$@CNTs-COOH with different numbers (1, 5, 10, 15, 20, 25 and 30).

Table S1 The atomic fractions of C, N, O and Si elemental for CF-$Cu(OH)_2$, CF-$Cu(OH)_2$@CNTs-NH_2 and CF-$Cu(OH)_2$@CNTs-COOH.

Table S2 The intrusion pressures and the oil column heights of 30 pieces of CF-$Cu(OH)_2$@CNTs-NH_2 and 25 pieces of CF-$Cu(OH)_2$@CNTs-COOH contacting toluene and 1,2-dichloroethane.

Movie S1 The SDS-T/W emulsion is separated by 30 pieces of CF-$Cu(OH)_2$@CNTs-NH_2.

Movie S2 The DTAC-T/W emulsion is separated by 25 pieces of CF-$Cu(OH)_2$@CNTs-COOH.

Movie S3 The SDS aqueous solution is filtered by 30 pieces of CF-$Cu(OH)_2$@CNTs-NH_2.

Movie S4 The DTAC aqueous solution is filtered by 25 pieces of CF-$Cu(OH)_2$@CNTs-COOH.

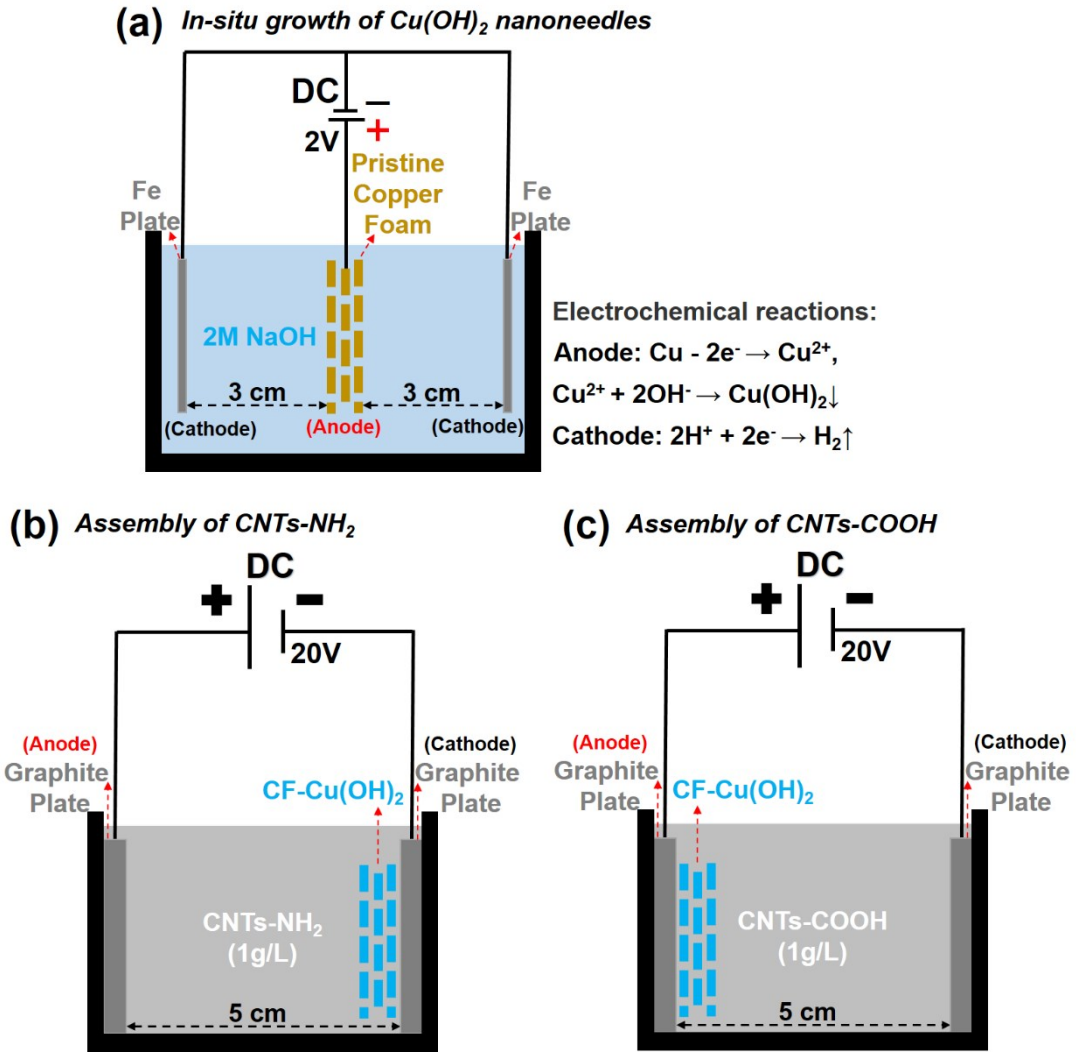

Fig. S1 Schematic representation for (a) preparation of CF-$Cu(OH)_2$ *via* a three-electrode anodization reaction and the corresponding electrochemical reaction equation. Schematic representation of directional electric field driven assembly method for (b) preparation of CF-$Cu(OH)_2$@CNTs-NH_2 *via* the assembly of CNTs-NH_2 on CF-$Cu(OH)_2$ and (c) preparation of CF-$Cu(OH)_2$@CNTs-COOH *via* the assembly of CNTs-COOH on CF-$Cu(OH)_2$.

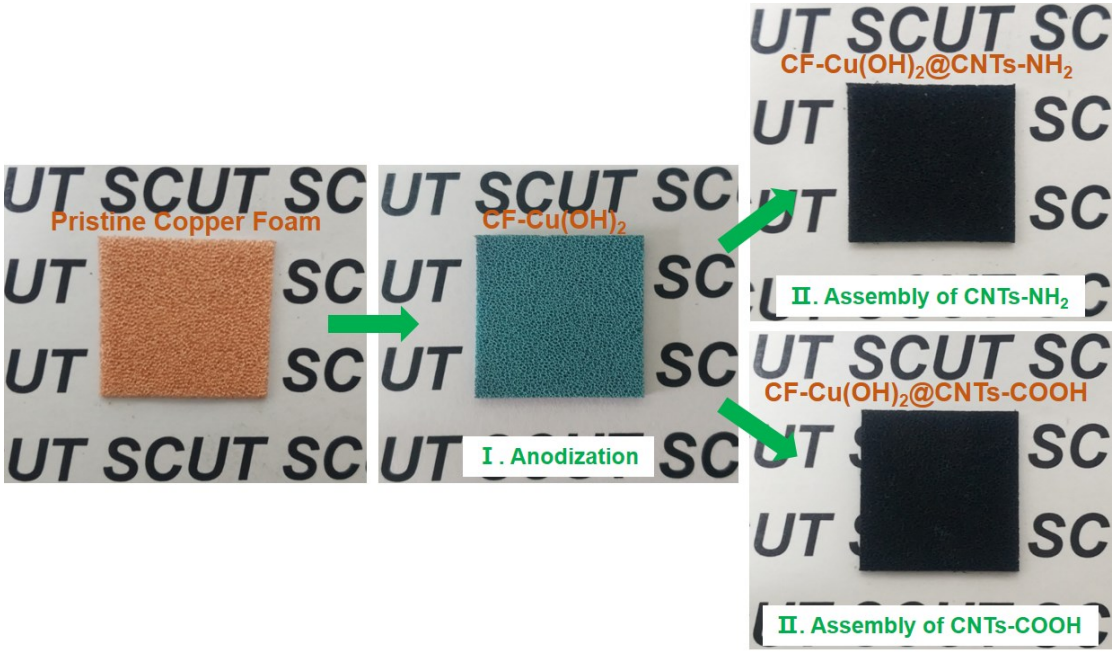

Fig. S2 Digital pictures of the pristine copper foam, CF-$Cu(OH)_2$, CF-$Cu(OH)_2$@CNTs-NH_2 and CF-$Cu(OH)_2$@CNTs-COOH.

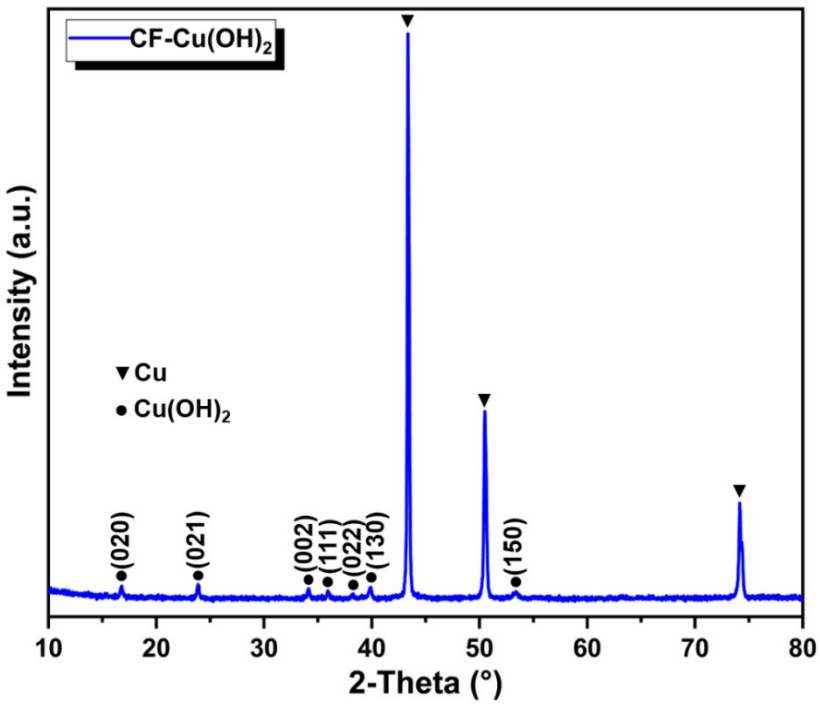

Fig. S3 XRD pattern of the CF-$Cu(OH)_2$.

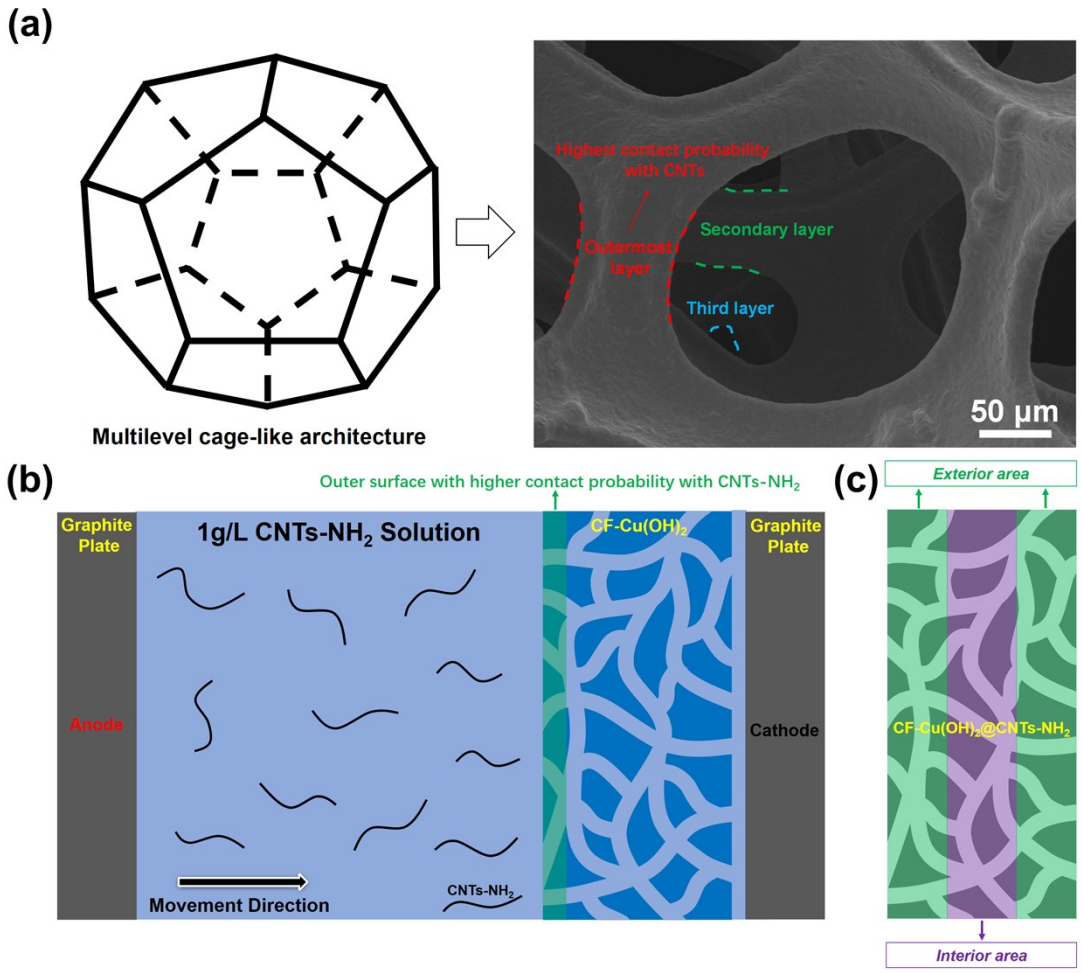

Fig. S4 (a) The SEM image of multilevel cage-like architecture for the copper foam. (b) Schematic illustration of the assembly of CNTs-NH_2 on the CF-$Cu(OH)_2$ *via* directional electric field driven assembly method. (c) The diagram of exterior area and interior area of the CF-$Cu(OH)_2$@CNTs-NH_2.

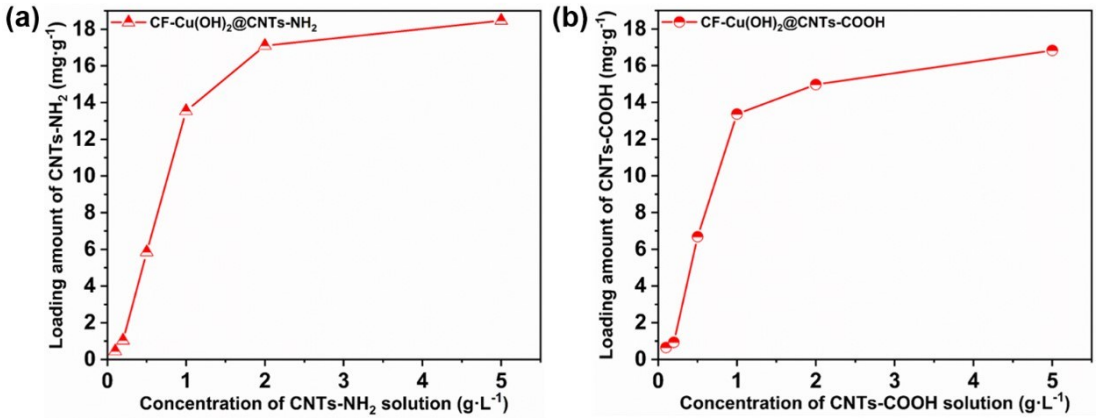

Fig. S5 The effect of concentration of CNTs solution on loading amount of CNTs of the (a) CF-$Cu(OH)_2$@CNTs-NH_2 and (b) CF-$Cu(OH)_2$@CNTs-COOH (The electric field assembly

time of CF-Cu(OH)$_2$@CNTs-NH$_2$ and CF-Cu(OH)$_2$@CNTs-COOH were fixed at 15 min and 5 min, respectively).

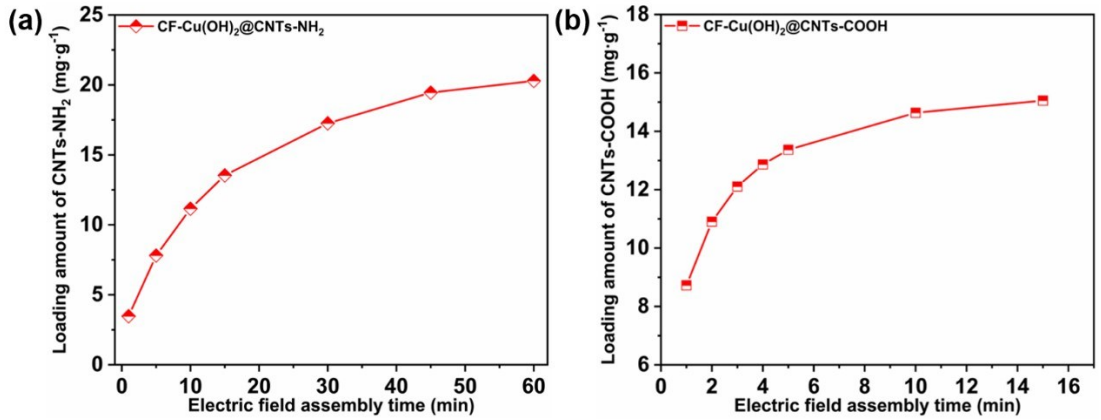

Fig. S6 The effect of electric field assembly time on loading amount of CNTs of the (a) CF-Cu(OH)$_2$@CNTs-NH$_2$ and (b) CF-Cu(OH)$_2$@CNTs-COOH (The concentrations of CNTs-NH$_2$/ CNTs-COOH solution in the assembly process for CF-Cu(OH)$_2$@CNTs-NH$_2$ and CF-Cu(OH)$_2$@CNTs-COOH were all fixed at 1 g·L^{-1}).

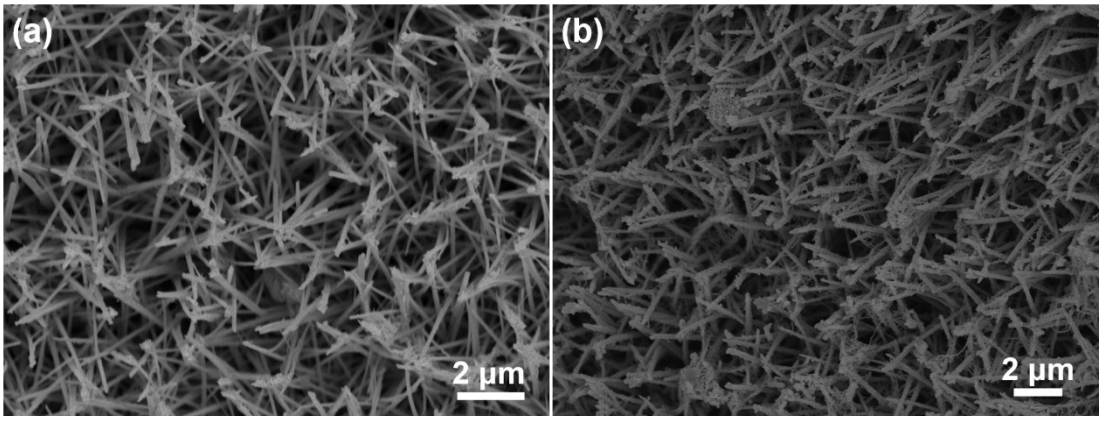

Fig. S7 SEM images of (a) CF-Cu(OH)$_2$@CNTs-NH$_2$ assembled with 0.1 g·L^{-1} CNTs-NH$_2$ solution for 15 min, (b) CF-Cu(OH)$_2$@CNTs-COOH assembled with 0.1 g·L^{-1} CNTs-COOH solution for 5 min.

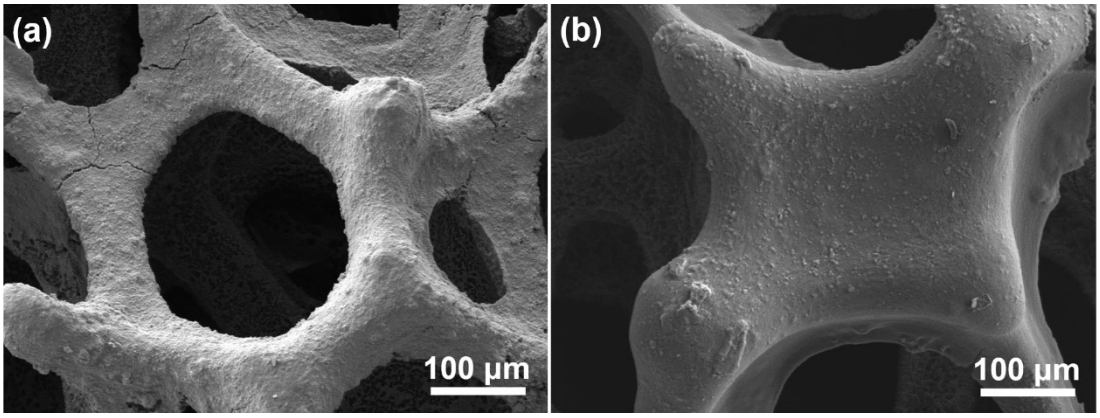

Fig. S8 SEM images of (a) CF-$Cu(OH)_2$@CNTs-NH_2 assembled with 5 $g \cdot L^{-1}$ CNTs-NH_2 solution for 15 min, (b) CF-$Cu(OH)_2$@CNTs-COOH assembled with 5 $g \cdot L^{-1}$ CNTs-COOH solution for 5 min.

Supplementary results and discussion

During the preparation of copper foams, the surface morphology will be affected by the concentration of CNTs solution and the electric field assembly time. If the concentration of CNTs-NH_2/CNTs-COOH solution is too low or the electric field assembly time is too short, the assembly density of CNTs-NH_2/CNTs-COOH on the copper foams will be very small. On the contrary, If the concentration of CNTs-NH_2/CNTs-COOH solution is too high or the electric field assembly time is too long, the assembly density of CNTs-NH_2/CNTs-COOH on the copper foams will be relatively dense. Too low assembly density of CNTs-NH_2/CNTs-COOH will result in a small number of CNTs-NH_2/CNTs-COOH on copper foam, which is very unfavorable for demulsification. Too high assembly density of CNTs-NH_2/CNTs-COOH will cause an excess of CNTs-NH_2/CNTs-COOH on the copper foam. The assembly density of CNTs-NH_2/CNTs-COOH was calculated by the loading amount of CNTs-NH_2/CNTs-COOH in this work, and the weights of copper foam before and after assembling CNTs-NH_2/CNTs-COOH were weighed by ultra-micro balance (Mettler Toledo XPR10/AC, Switzerland). For CF-$Cu(OH)_2$@CNTs-NH_2, when the concentration of CNTs-NH_2 solution is as low as 0.1 $g \cdot L^{-1}$ with the electric field assembly time fixed at 15 min, the loading amount of CNTs-NH_2 is only 0.453 $mg \cdot g^{-1}$ (Fig. S5a), and the number of CNTs-NH_2 in the exterior area is very small under SEM observation (Fig. S7a). When the concentration of CNTs-NH_2 solution increases gradually, the loading amount of CNTs-NH_2 also increases, and the loading amount reaches 13.543 $mg \cdot g^{-1}$ at 1 $g \cdot L^{-1}$ of the CNTs-NH_2 concentration. After further increasing the

concentration of CNTs-NH_2 solution, after which the growth rate of loading amount of CNTs-NH_2 on copper foam gradually slows down. This is because the $Cu(OH)_2$ nanoneedles have been completely covered by a certain amount of CNTs-NH_2, and excessive CNTs-NH_2 cannot be combined with $Cu(OH)_2$ nanoneedles through electrostatic bonding and disorderly winding fixation. As we can see from Fig. S8a, the whole pentagonal cage-like skeleton is thickly wrapped by CNTs-NH_2. Unfortunately, once the CNTs-NH_2 layer is piled up too heavy, part of the area will be cracked due to the inability to bear the weight. The loading amount of CNTs-COOH shows the same change trend when the electric field assembly time of CF-$Cu(OH)_2$@CNTs-COOH is fixed at 5 min (Fig. S5b and S7b). Furthermore, Fig. S6 shows the loading amount of CNTs-NH_2/CNTs-COOH as a function of electric field assembly time. The loading amount of CNTs-NH_2/CNTs-COOH of CF-$Cu(OH)_2$@CNTs-NH_2 and CF-$Cu(OH)_2$@CNTs-COOH can be assembled to 3.471 and 8.722 $mg \cdot g^{-1}$ within 1 min, respectively. Then the loading amount of CNTs-NH_2/CNTs-COOH increases with the extension of electric field assembly time, but the increasing trend is also gradually slowing down. Because as the CNTs-NH_2/CNTs-COOH are immobilized on the $Cu(OH)_2$ nanoneedles, the charge sites for electrostatic attraction are also reduced, and the positions on the $Cu(OH)_2$ nanoneedles are gradually occupied by the CNTs-NH_2/CNTs-COOH. As the electric field assembly proceeds, the number of CNTs-NH_2/CNTs-COOH that can be immobilized by the $Cu(OH)_2$ nanoneedles is gradually decreased.

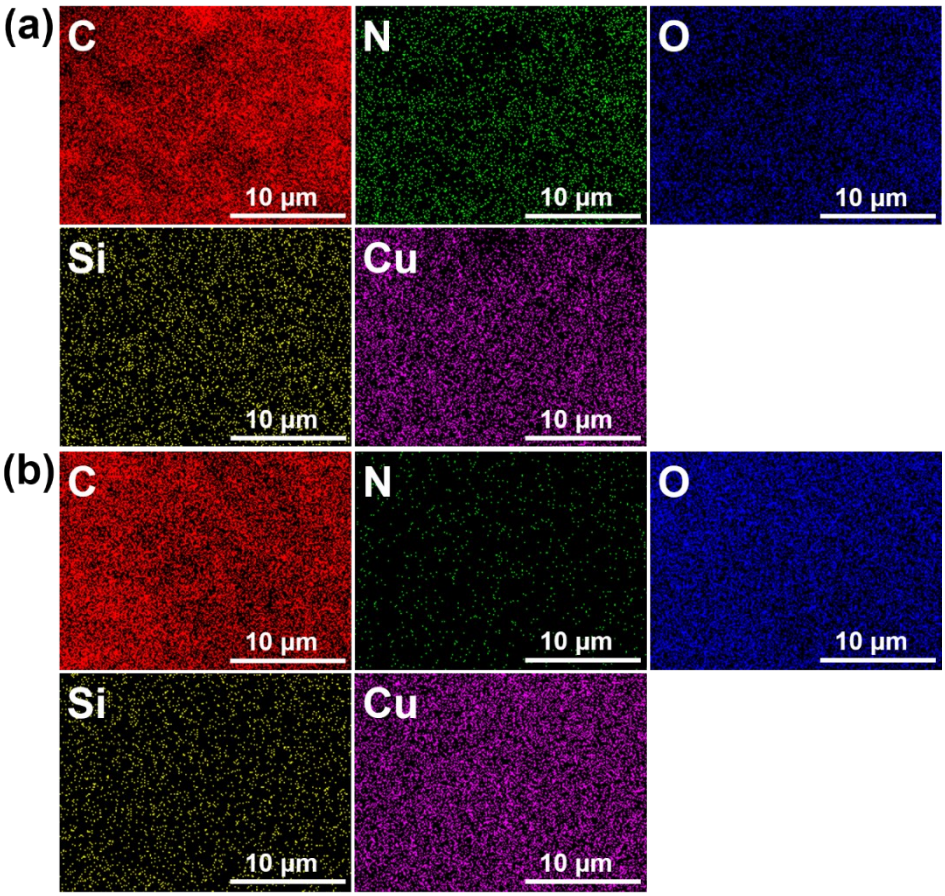

Fig. S9 The EDS mapping for (a) CF-Cu(OH)$_2$@CNTs-NH$_2$ and (b) CF-Cu(OH)$_2$@CNTs-COOH.

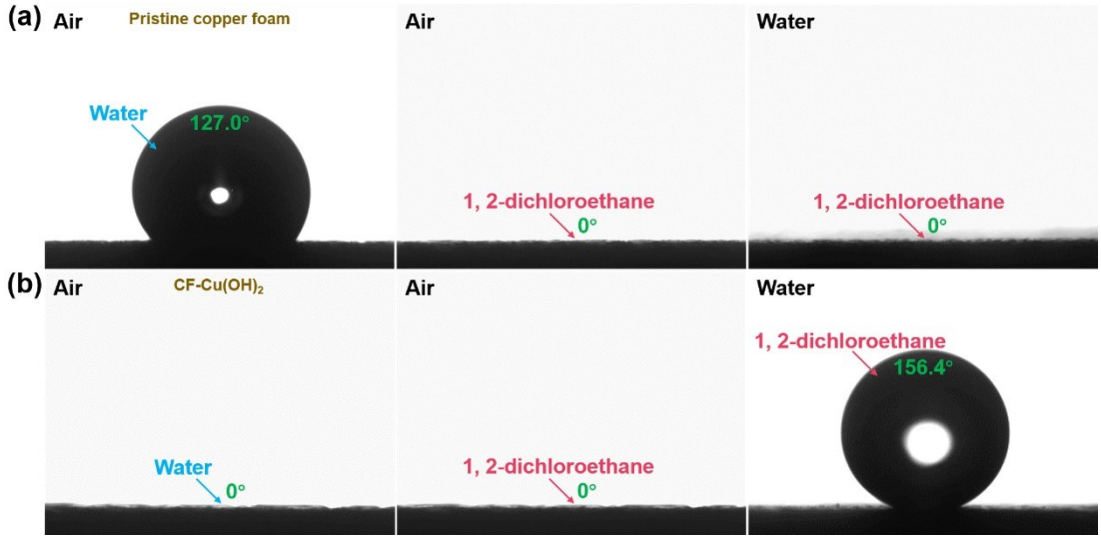

Fig. S10 The water contact angle (WCA), oil contact angle (OCA) and underwater oil contact angle (UWOCA) of (a) pristine copper foam and (b) CF-Cu(OH)$_2$.

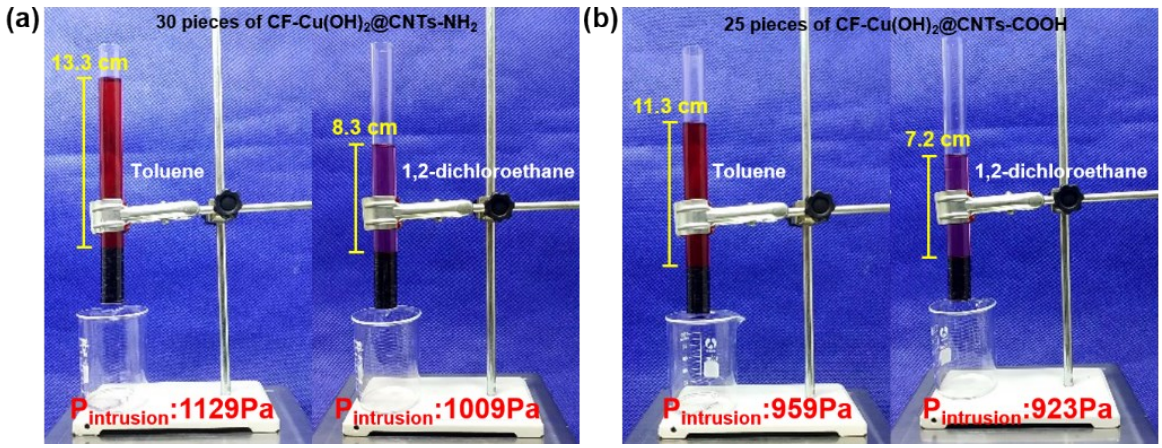

Fig. S11 The measurement of oil intrusion pressures of 30 pieces of CF-Cu(OH)$_2$@CNTs-NH$_2$ and 25 pieces of CF-Cu(OH)$_2$@CNTs-COOH (Oil are toluene (red) and 1,2-dichloroethane (purple)).

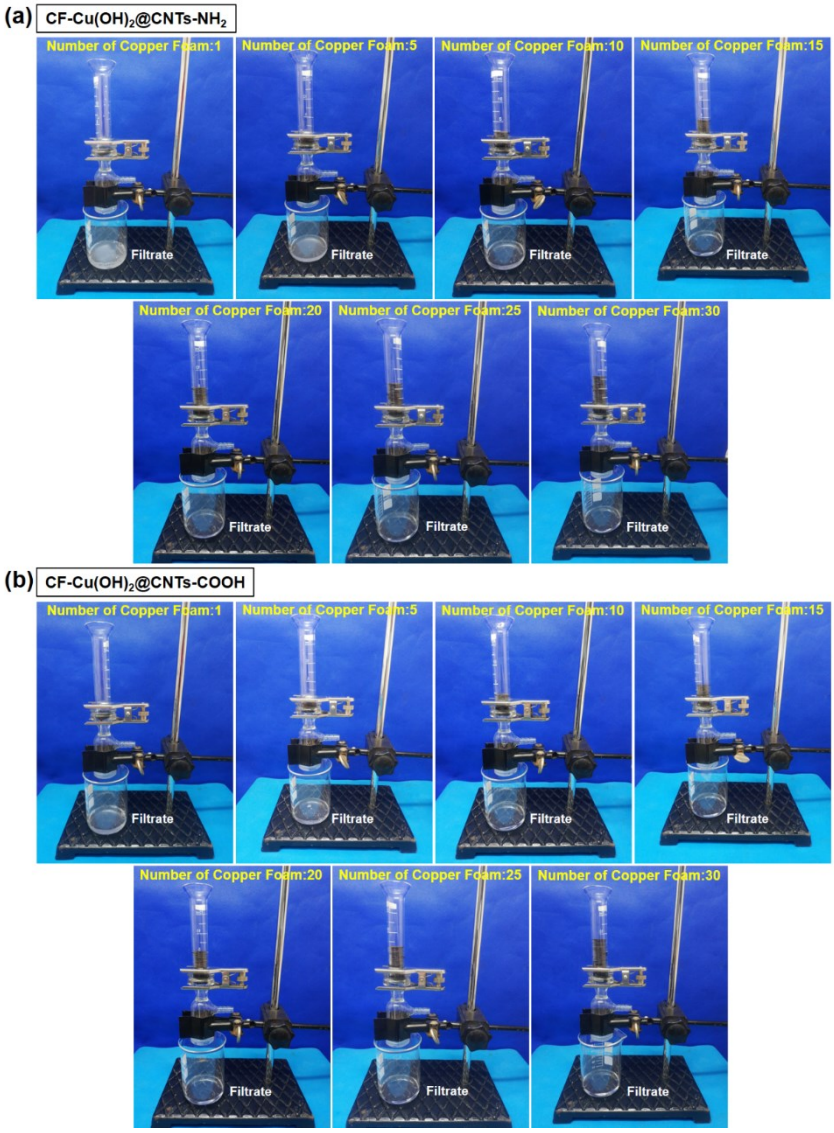

Fig. S12 (a) The appearance of the filtrates for SDS-T/W emulsion separated by CF-

$Cu(OH)_2$@CNTs-NH_2 with different numbers (1, 5, 10, 15, 20, 25 and 30). (b) The appearance of the filtrates for DTAC-T/W emulsion separated by CF-$Cu(OH)_2$@CNTs-COOH with different numbers (1, 5, 10, 15, 20, 25 and 30).

Table S1

The atomic fractions of C, N, O and Si elemental for CF-$Cu(OH)_2$, CF-$Cu(OH)_2$@CNTs-NH_2 and CF-$Cu(OH)_2$@CNTs-COOH.

Material type	C (%)	N (%)	O (%)	Si (%)	Total
CF-$Cu(OH)_2$	22.56	-	77.44	-	100.00
CF-$Cu(OH)_2$@CNTs-NH_2	67.00	14.29	15.79	2.92	100.00
CF-$Cu(OH)_2$@CNTs-COOH	63.48	3.99	28.73	3.80	100.00

Table S2

The intrusion pressures and the oil column heights of 30 pieces of CF-$Cu(OH)_2$@CNTs-NH_2 and 25 pieces of CF-$Cu(OH)_2$@CNTs-COOH contacting toluene and 1,2-dichloroethane.

Material type	Oil column height (cm)		Intrusion pressure (Pa)	
	Toluene	1,2-dichloroethane	Toluene	1,2-dichloroethane
30 pieces of CF-$Cu(OH)_2$@CNTs-NH_2	13.3	8.3	1129	1009
25 pieces of CF-$Cu(OH)_2$@CNTs-COOH	11.3	7.2	959	923